Mobile element integration reveals an atypical chromosome dimer resolution system in *Legionella pneumophila*

Beth Nicholson[1], Shayna R. Deecker[1] and Alexander W. Ensminger[1,2]#

[1] Department of Biochemistry, University of Toronto, Toronto, Ontario, Canada.

[2] Department of Molecular Genetics, University of Toronto, Toronto, Ontario, Canada.

Running title: Chromosome dimer resolution in *Legionella*

#Address correspondence to Alexander W. Ensminger, alex.ensminger@utoronto.ca

Keywords: *Legionella pneumophila*, chromosome dimer resolution, site-specific recombination, Xer, *dif,* IMEX

ABSTRACT

In bacteria, the mechanisms used to repair DNA lesions during genome replication include homologous recombination between sister chromosomes. This can lead to the formation of chromosome dimers if an odd number of crossover events occurs. The concatenated DNA must be resolved before cell separation to ensure genomic stability and cell viability. The broadly conserved *dif*/Xer system counteracts the formation of dimers by catalyzing one additional crossover event immediately prior to cell separation. While *dif*/Xer systems have been characterized or predicted in the vast majority of proteobacteria, no homologs to *dif* or *xer* have been identified in the order *Legionellales*. Here we report the discovery of a distinct *dif*/Xer system in the intracellular pathogen *Legionella pneumophila*. The *dif* site was uncovered by our analysis of *Legionella* mobile element-1 (LME-1), which harbors a *dif* site mimic and integrates into the *L. pneumophila* genome via site-specific recombination. We demonstrate that *lpg1867* (herein named *xerL*) encodes a tyrosine recombinase that is necessary and sufficient for catalyzing recombination at the *dif* site, and that deletion of *dif* or *xerL* causes filamentation and slow growth phenotypes. In addition, our data show that LME-1 can be classified as an integrative mobile element exploiting Xer (IMEX). The identification of LME-1 as an IMEX of *Legionella*'s atypical *dif*/Xer system further highlights the extent to which diverse mobile elements have independently evolved to exploit this critical cellular machinery.

34 **INTRODUCTION**

35 The circular nature of bacterial chromosomes brings about a problem for the partitioning of
36 genetic information to daughter cells: the formation of chromosome dimers during replication.
37 Dimers are generated when homologous recombination-mediated repair of DNA lesions results in an
38 odd number of crossover events between sister chromosomes. The concatenated DNA must be
39 resolved into monomers for proper cell division to occur. The essential and broadly conserved
40 bacterial *dif*/Xer system overcomes this topological problem by catalyzing one additional crossover
41 event immediately prior to cell separation (Barre et al., 2001; Steiner & Kuempel, 1998). The *dif*
42 (deletion-induced filamentation) site is a conserved ~30-bp DNA element on the chromosome that
43 contains binding sites for either two copies of a single tyrosine recombinase or one copy of two
44 different ones (Blakely et al., 1991, 1993; Castillo et al., 2017; Le Bourgeois et al., 2007; Leroux et
45 al., 2013; Sciochetti et al., 2001). In a highly regulated process, a nucleoprotein complex containing
46 the Xer tetramer and two aligned *dif* sites forms a recombination synapse, and site-specific
47 recombination between them deconcatenates the chromosome dimer into monomers (Thanbichler,
48 2010).

49 Dimer resolution via site-specific recombination by tyrosine recombinases was first
50 discovered in plasmids (Austin et al., 1981; Summers & Sherratt, 1984) including ColE1, in which a
51 DNA sequence named *cer* was found to be essential for plasmid monomerization and stability
52 (Summers & Sherratt, 1984). Recombination between *cer* sites was later found to require catalysis
53 by XerC (Colloms et al., 1990) and XerD (Blakely et al., 1993) encoded on the *E. coli* genome.
54 These findings, along with homology between the chromosomal *dif* site and *cer*, led to the discovery

55 of the *dif*/XerCD chromosome dimer resolution (CDR) pathway in *E. coli* (Blakely et al., 1991,
56 1993; Clerget, 1991; Kuempel et al., 1991) and later in several other species of bacteria (Debowski
57 et al., 2012; Jensen, 2006; Le Bourgeois et al., 2007; Leroux et al., 2013; Sciochetti et al., 2001; Val
58 et al., 2008) and archaea (Cortez et al., 2010; Duggin et al., 2011). Subsequent dissection of the
59 *dif*/Xer recombination machinery has been aided by another group of mobile genetic elements,
60 named integrative mobile elements exploiting Xer (IMEX) (Das et al., 2011, 2013; Fournes et al.,
61 2016; Hassan et al., 2010; Huber & Waldor, 2002; Midonet et al., 2014; Midonet & Barre, 2014; Val
62 et al., 2005). IMEXs, which include lysogenic phages, genomic islands, and plasmids, contain a *dif*-
63 mimic sequence which allows them to integrate into the chromosome at the *dif* site using the host's
64 Xer recombination machinery (Das et al., 2013; Midonet & Barre, 2014).

65 Homologs of *xerC* and *xerD* have been predicted to be present in the vast majority of
66 proteobacterial species (Carnoy & Roten, 2009). Exceptions to this include two groups of bacteria
67 that utilize a single-recombinase system. The *Streptococci*/*Lactococci* use a single recombinase XerS
68 and an atypical *dif* site (Le Bourgeois et al., 2007) and a group of epsilon-proteobacteria, including
69 *Helicobacter* and *Campylobacter* species, uses a single-recombinase XerH system (Carnoy & Roten,
70 2009). While *dif*/Xer homologs have been detected in almost 90% of proteobacteria, no *dif* or Xer
71 homologs could be detected in the order *Legionellales*, despite encoding RecA, RecBCD, and RecF,
72 which are thought to be responsible to dimer formation during replication (Carnoy & Roten, 2009).
73 How then do the members of the order *Legionellales* overcome the threat to genome stability that
74 chromosome dimers impose? It is possible that they use an entirely different method for CDR, or
75 that its *dif*/Xer system is sufficiently divergent from others to avoid detection by sequence-based
76 homology searches.

77 Several strains of *Legionella pneumophila* harbor a phage-like integrative mobile genetic
78 element, named *Legionella* mobile element-1 (LME-1) (Deecker et al., 2021; Lüneberg et al., 2001;
79 Rao et al., 2016). We previously found that integration into the genome requires a 22-bp attachment
80 site (*att*) in LME-1 that is identical to a sequence on the *L. pneumophila* genome (Rao et al., 2016).
81 Even though LME-1 is only integrated in a small proportion of sequenced *L. pneumophila* isolates,
82 the chromosomal *att* site is present in all *L. pneumophila* isolates and *Legionella* species described to
83 date (Table S1), a level of conservation that suggests an important function. We report here that the
84 LME-1 *att* site on the chromosome meets several criteria of the missing *dif* site in *Legionella*: size
85 ~30 bp, low GC-content, some degree of palindromicity, positioned close to the replication terminus,
86 and in a non-coding region with varying flanking genes. We identify a single recombinase that is
87 both necessary and sufficient for site-specific recombination at this site. Together, our results
88 suggest that *L. pneumophila* uses a distinct single-recombinase system for CDR and that LME-1 is
89 an IMEX of that system.
90
91 **RESULTS**
92 **The LME-1 attachment site is invariably close to the *Legionella* replication terminus.**
93 We previously determined that LME-1 integrates into the *L. pneumophila* genome via a 22-
94 bp attachment (*att*) site (Rao et al., 2016). The corresponding *att* site on the chromosome is
95 contained within a broader 29-bp sequence that is conserved across all sequenced *L. pneumophila*
96 strains and *Legionella* species (**Fig. 1A, Table S1**), suggesting that it performs an essential function.
97 While the *att* site itself is conserved, its genomic neighbourhood varies (Rao et al., 2016) (**Table**
98 **S1**), indicating that the intrinsic function of this sequence may be unrelated to its flanking genes. In a
99 search for attributes of the *att* site that may hint at its function, we analyzed its chromosomal
100 location in all *L. pneumophila* strains with available genome sequences (**Table S1**). We found that

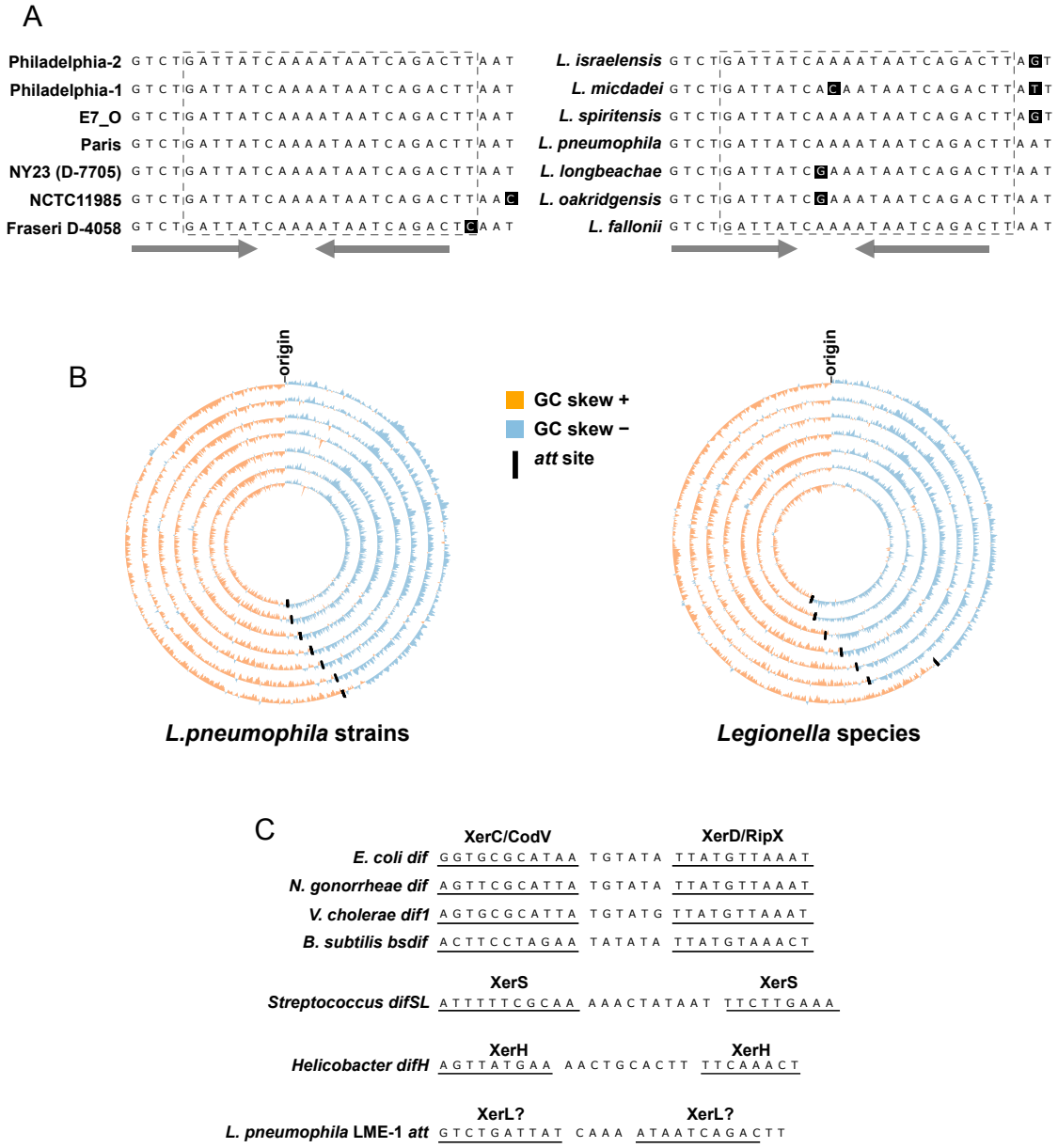

Figure 1 | The DNA sequence hijacked by LME-1 is invariably proximal to the site of GC-skew inflection and resembles a *dif* site. A) Sequence alignment of the LME-1 *att* site region in different *L. pneumophila* strains (left panel) and other *Legionella* species (right panel). The dashed-line box denotes the 22-nt sequence that corresponds to the *att* site present on LME-1. The grey arrows indicate the inverted repeat portion of the sequence. **B)** Circos plots showing GC-skew across the chromosome of several *L. pneumophila* strains (left panel) and other *Legionella* species (right panel). Each ring corresponds to one genome, with inside-to-outside rings corresponding to the genomes listed top-to-bottom in the alignments in panel A. The black line indicates the position of the *att* site in each genome. **C)** Alignment of the LME-1 *att* site with *dif* sites from bacterial species with established *dif*/Xer systems. The binding sites for XerC and XerD homologs (named CodV and RipX, respectively in *B. subtilis*) (Blakely et al., 1991, 1993; Sciochetti et al., 2001), XerS (Nolivos et al., 2010), and XerH (Bebel et al., 2016; Leroux et al., 2013) are underlined.

101 despite the disparate gene neighbourhoods, the location of the *att* site was roughly opposite the
102 origin of replication in all cases. In fact, GC-skew analysis of each genome revealed that the *att* site
103 was invariably close to the cumulative GC-skew maximum, which occurs at the site of replication
104 termination (Grigoriev, 1998) (**Fig. 1B, Table S1**). The *att* site is present within a small ~8-kb
105 window between 35 kb and 43 kb from the GC-skew inflection point (**Table S1**). This specificity of
106 positioning extended to the *att* sites of other *Legionella* species, which are located between 89 bp
107 and 79 kb from the point of GC-skew inflection (**Fig. 1B, Table S1**).
108 The proximity of the LME-1 *att* site to the terminus region is reminiscent of bacterial *dif*
109 sites, so we next compared the *att* site to the *dif* sites of several bacteria with established *dif*/Xer
110 systems. In addition to its proximity to the terminus, the LME-1 *att* site shows several similarities to
111 known *dif* sites, including (i) intergenic location (**Table S1**), (ii) size of ~30 bp, (iii) low G+C
112 content, and (iv) a short central region flanked by left and right arms with some degree of dyad
113 symmetry (**Fig. 1C**). However, the LME-1 *att* site is distinguished from known *dif* sites by the
114 perfect dyad symmetry of its 10-bp arms and the short 4-bp central region separating them. The arms
115 do not show homology to any known Xer-binding motifs (**Fig. 1C**) (Carnoy & Roten, 2009).
116

117 **The *L. pneumophila dif* site supports highly efficient RecA-independent DNA recombination.**

118 The similarities between the chromosomal LME-1 *att* site (hereafter referred to as the
119 *Legionella dif* site) and established *dif* sites suggest that it likely contains two binding sites for one or
120 more tyrosine-type recombinases that catalyze site-specific recombination (Castillo et al., 2017). To
121 assess the ability of the *L. pneumophila dif* site to undergo site-specific recombination, we used an
122 intermolecular recombination assay (**Fig. 2A**). In this assay, a non-replicative plasmid (pJB4648)
123 containing a gentamicin-resistance marker and a 22-bp portion of the *dif* site (corresponding to the
124 LME-1 *att* site) is transformed into *L. pneumophila* strain Lp02. If site-specific recombination
125 occurs between the *att* site on the plasmid and the chromosomal *dif* site, the entire plasmid will be

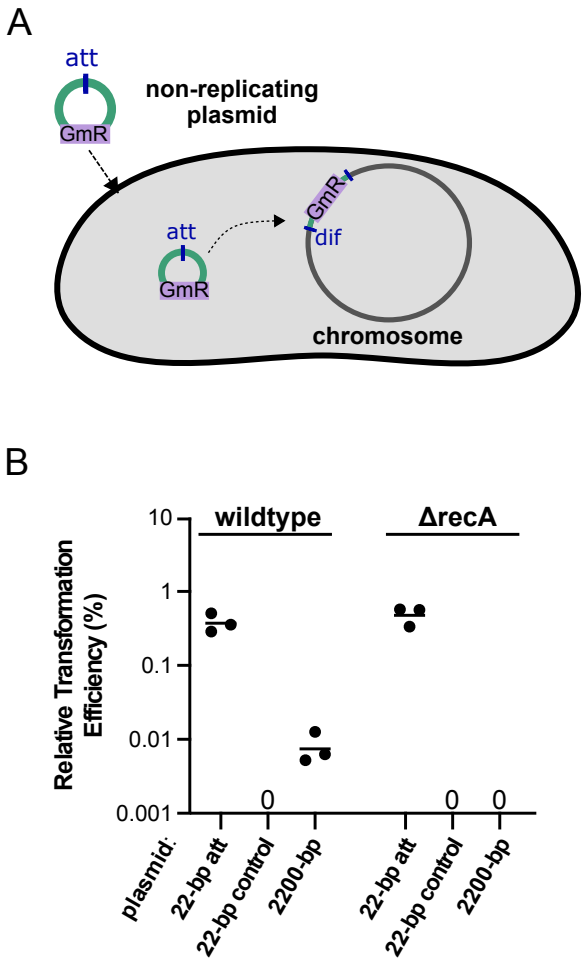

Figure 2 | Site-specific recombination at the *dif* site is highly efficient and does not require RecA. A) Schematic representation of the intermolecular recombination assay used to quantify *att* site-specific recombination in *L. pneumophila*. A 5.5-kb non-replicating plasmid modified to include the 22-bp LME-1 *att* site (or control sequences) is transformed into *L. pneumophila* strain Lp02. If recombination between the plasmid *att* site and the chromosomal *dif* site takes place, the whole plasmid is integrated into the genome and gentamicin resistance is conferred to the cell. Gentamicin-resistant colonies are counted to quantify recombination. **B)** Shown is the transformation efficiency (relative to that of a replicative plasmid control) of a non-replicative plasmid containing the 22-bp *att* site, a 22-bp control sequence, or a 2200-bp intergenic region of the Lp02 genome, transformed into wildtype or Δ*recA* Lp02 strains. Each dot shows the value obtained from a single experiment, and each horizontal line represents the geometric mean of 3 independent experiments.

integrated into the genome and confer gentamicin resistance to the cell. We compared the number of transformants resulting from the *att*-containing plasmid to one with a control 22-bp sequence derived from the *L. pneumophila* genome near the *dif* site. To evaluate the efficiency of recombination supported by the *dif* site, we also included a plasmid containing 2200 bp of unrelated intergenic sequence from *L. pneumophila*, which can integrate into the genome via a single-crossover homologous recombination event. Considering that chromosomal *dif* site-specific recombination is known to be RecA-independent (Domínguez et al., 2011; Kuempel et al., 1991; Le Bourgeois et al., 2007), we also assessed the integration of each of these plasmids in a *recA* deletion strain (**Fig. 2B**). To control for any strain-to-strain differences in overall transformation efficiency, we normalized the number of transformants for each plasmid to the number resulting from transformation with a replicative plasmid (pJB1806_GmR). The *att* site-containing plasmid integrated into the genome at a

137 high rate, with an efficiency that was 50-fold higher than that of the 2200-bp control. In contrast, the
138 22-bp control sequence did not generate any transformants, indicating that the number of integration
139 events was lower than the detection limit of 1 CFU per ~2×10^9 cells. In the Δ*recA* strain, no
140 transformants were detected for the 2200-bp control which relies on homologous recombination for
141 integration, while the *att* site-containing plasmid integrated at a level similar to that in the wildtype
142 strain (**Fig. 2B**). In both the wildtype and Δ*recA* strains, integration of the *att*-containing plasmid at
143 the chromosomal *dif* site was confirmed by PCR-amplification of the *dif* region and Sanger
144 sequencing (data not shown). These data indicate that, similar to other *dif* sites, site-specific
145 recombination at the *L. pneumophila dif* site is efficient and recA-independent.
146
147 ***Legionella* Xer/*dif* is likely a single-recombinase system.**
148 We next aimed to identify the recombinases that catalyzes recombination at the *Legionella*
149 *dif* site. No orthologs of XerC, XerD, XerS, or XerH have been identified in *Legionella* using
150 sequence homology (Carnoy & Roten, 2009). However, HHPred analysis revealed that six *L.*
151 *pneumophila* genes present in strain Lp02 (*lpg0980*, *lpg0981*, *lpg1070*, *lpg1085*, *lpg1867*, and
152 *lpg2057*) show structural similarity to tyrosine-type recombinases (probability >99%). We therefore
153 repeated our intermolecular recombination assay in strains containing individual deletions of these
154 six genes, along with a strain lacking the *dif* site. As expected, deletion of the *dif* site resulted in no
155 detectable integration of the *att* site-containing plasmid. Deletion of *lpg1867* also specifically
156 abolished integration, while deletion of each of the other five recombinases had no significant effect
157 (**Fig. 3A**). We also performed rescue experiments using expression plasmids to confirm that the loss
158 of recombination at the *dif* site in the Δ*lpg1867* strain was due to loss of Lpg1867 protein function
159 and not any secondary mutations acquired during strain generation. Expression of Lpg1867 in the
160 Δ*lpg1867* strain resulted in near-wildtype levels of recombination (**Fig. 3B**). In contrast, no
161 recombination was detected with an empty vector control or when a point mutant of Lpg1867

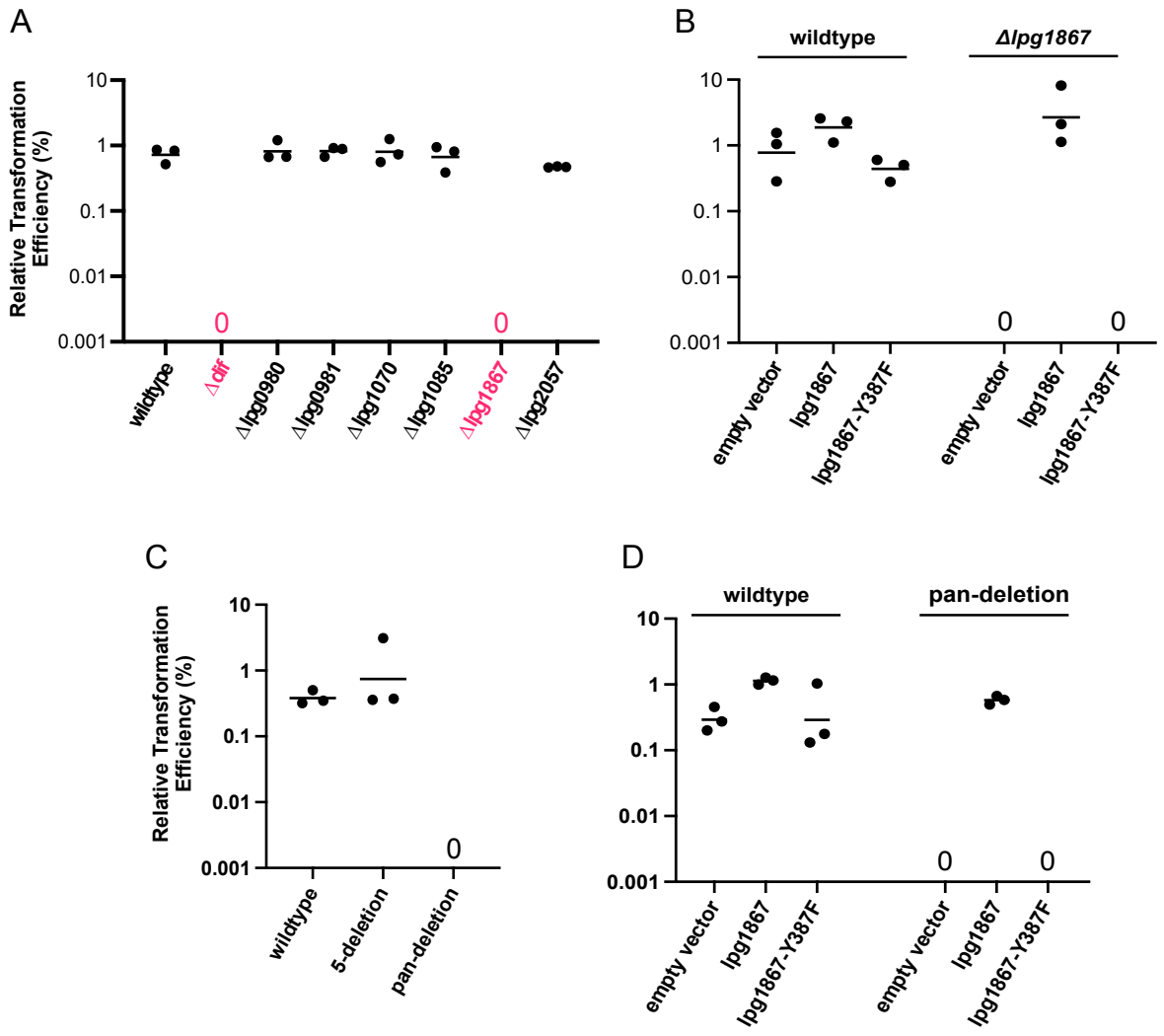

Figure 3 | The *L. pneumophila* Xer is encoded by *lpg1867* and does not require a partner recombinase. Shown are dot plots for assays detecting intermolecular recombination between a plasmid containing the 22-bp *att* site and the chromosomal *dif* site, as described for Figure 2. **A)** Intermolecular recombination in wildtype Lp02 and strains containing deletions of the *dif* site or one of six tyrosine-type recombinases. Shown in pink are the *dif*-deletion strain and *lpg1867*-deletion strain, which both displayed levels of recombination below the limit of detection. **B)** The wildtype and Δ*lpg1867* strains were transformed with plasmids expressing wildtype Lpg1867 or a predicted catalytic point mutant, Y387F. Wildtype Lpg1867, but not the catalytic mutant, rescued the recombination defect in the Δ*lpg1867* strain. **C)** Recombination in the wildtype strain was compared to that in a 5-deletion strain (*lpg0980*, *lpg0981*, *lpg1070*, *lpg1085*, and *lpg2057* deleted) and a pan-deletion strain, with all six recombinases deleted (i.e, 5-deletion plus *lpg1867* deletion). **D)** The wildtype strain and pan-deletion strain were transformed with expression plasmids as in panel B. Wildtype Lpg1867, but not the catalytic mutant, fully rescued the recombination defect in the pan-deletion strain.

162 (Y387F) was expressed. The Y387F mutant is predicted to be catalytically inactive based on the
163 equivalent catalytic tyrosine mutation in other tyrosine recombinases (Blakely et al., 1993; Gibb et
164 al., 2010; Pan et al., 1993).

165 We next asked whether one of the other five putative tyrosine recombinases might be
166 involved along with Lpg1867 in recombination at the *dif* site, despite having no effect upon
167 individual deletion. To address this, we generated two multiple-deletion strains: one with five
168 putative recombinases deleted (all except *lpg1867*), and a pan-deletion strain with all six deleted. In
169 our intermolecular recombination assay, integration of the *att*-containing plasmid was similar to
170 wildtype levels in the 5-deletion strain and nonexistent in the pan-deletion strain (**Fig. 3C**).
171 Overexpression of Lpg1867, but not Lpg1867-Y387F, again rescued the recombination defect (**Fig.
172 3D**). Collectively, these data indicate that Lpg1867 is both necessary and sufficient to catalyze site-
173 specific recombination at the *L. pneumophila dif* site.

174

175 **Deletion of *dif* or *lpg1867* induces filamentation and inhibits growth.**

176 Loss of a functional chromosome dimer resolution system causes defects in cell division,
177 which can result in a variety of phenotypes including slow growth and filamentation (the *dif* site was
178 named for its deletion-induced filamentation phenotype). Consistent with reported findings for *dif* or
179 *xer* deletions in other species (Blakely et al., 1991; Debowski et al., 2012; Farrokhi et al., 2019;
180 Hendricks et al., 2000; Kuempel et al., 1991; Sciochetti et al., 2001), we observed that loss of *dif* or
181 Lpg1867 in *L. pneumophila* led to filamentation in a subpopulation of cells (**Fig. 4A**). Notably, and
182 consistent with a reduction in chromosome dimer formation in the absence of RecA (Pérals et al.,
183 2000; Steiner & Kuempel, 1998) we observed a decrease in filament formation upon deletion of
184 *recA* in the Δ*lpg1867* background (**Fig. 4A**).

185 Deletion of *dif* or *lpg1867* also results in a visible reduction in colony growth on solid media
186 (**Fig. 4B**). Again, this defect is alleviated upon additional deletion of *recA* in the *Δlpg1867*

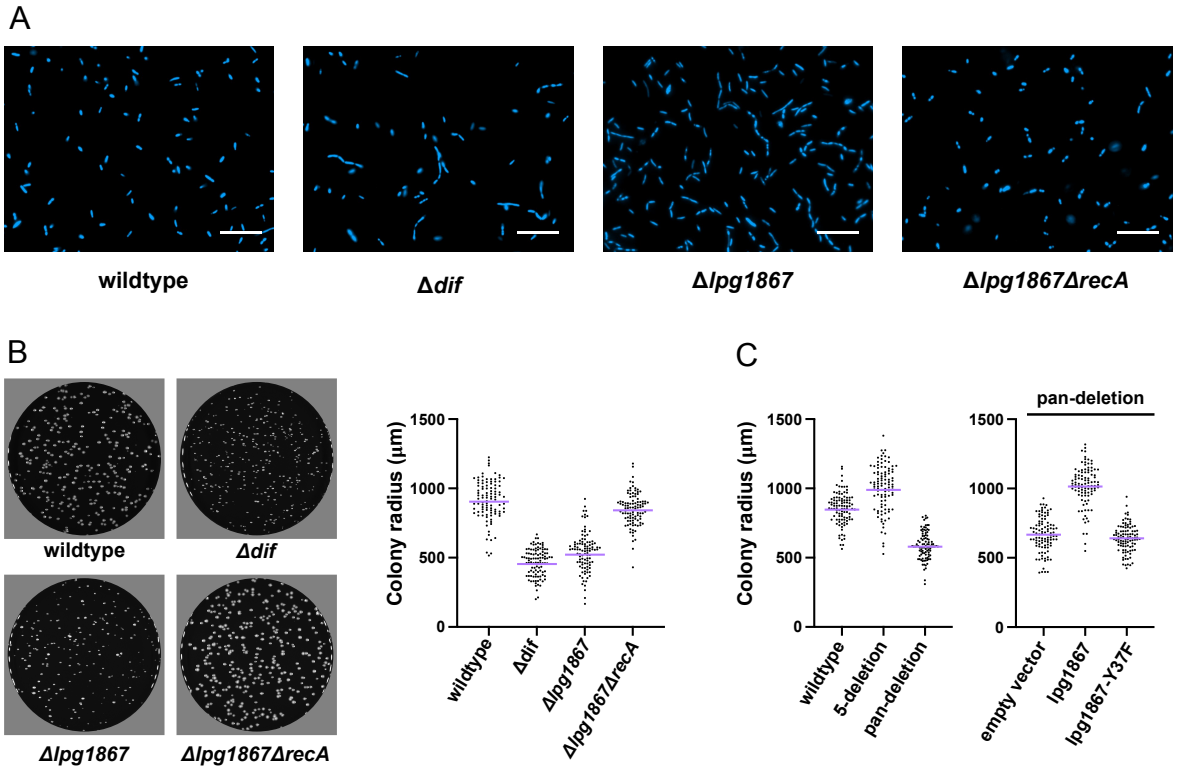

Figure 4 | *dif- and lpg1867*-deletion strains exhibit filamentation and altered growth on solid media. A) DAPI-stained cells of the indicated *L. pneumophila* strains, showing filamentation upon deletion of the *dif* site or *lpg1867* and rescue when *recA* is deleted in the Δ*lpg1867* background. The scale bars represent 10 µm. **B)** CYET spread plates after 4 days of growth at 37°C with visible differences in colony size (left panel). Each colony radius is plotted as a separate data point, with the geometric mean shown by the purple line (right panel). The reduction in colony size in the Δ*lpg1867* strain is rescued by the additional deletion of *recA*. **C)** Distribution of colony sizes in the 5-deletion strain and pan-deletion strain (left panel) and in the pan-deletion strain expressing wildtype or mutant Lpg1867 (right panel). Data are plotted as in panel B. Wildtype Lpg1867, but not the catalytic mutant Lpg1867-Y387F, rescues the small colony phenotype observed in the pan-deletion.

187 background (**Fig. 4B**), consistent with the growth inhibition being caused by an inability to resolve
188 chromosome dimers. The slow growth phenotype is also present in the recombinase pan-deletion
189 strain, but not the 5-deletion strain, and the defect is rescued by expression of wildtype Lpg1867 but
190 not the catalytic mutant (**Fig. 4C**), mirroring the effects of these deletions on recombination (**Fig.**
191 **3C,D**). Taken together, these data support a model in which a single site-specific recombinase,
192 Lpg1867 (which we designate here as XerL), catalyzes recombination between two *dif* sites to
193 resolve chromosome dimers in *Legionella*.
194

195 **LME-1 stability is modulated by Lpg1867 (XerL) and the formation of a modified downstream**
196 ***dif* site.**

197 We have previously shown that LME-1 integrates into the *L. pneumophila* chromosome at
198 what we now know to be the *dif* site (Rao et al., 2016). Other invasive elements known to integrate
199 at the *dif* site of their host (IMEXs) do not encode their own recombinase and instead utilize the host
200 Xer for integration/excision (Das et al., 2013; Midonet & Barre, 2014). Similarly, LME-1 does not
201 appear to encode its own recombinase or integrase (Deecker et al., 2021). Our intermolecular
202 recombination assay indicates that XerL can facilitate integration of circular DNA containing the
203 LME-1 22-bp *att* site (**Fig. 2, Fig. 3**). To investigate whether XerL is also involved in LME-1
204 excision, we overexpressed XerL in *L. pneumophila* strain Murcia-4983, which naturally contains
205 LME-1 stably integrated at its *dif* site (Rao et al., 2016). Using an established qPCR-based assay
206 (Rao et al., 2016), we quantified LME-1 excision in this strain upon XerL overexpression and found
207 that excision was increased >25 fold compared to a control strain transformed with empty vector
208 (**Fig. 5A**). Interestingly, the catalytic mutant Lpg1867-Y387F did not enhance excision, and in fact
209 inhibited excision by >5 fold (**Fig. 5A**). A possible explanation for this is that the mutant Lpg1867 is
210 acting as a dominant-negative by binding the *dif/att* sites but not catalyzing recombination.

211 LME-1 is stably integrated into the Murcia-4983 genome (only excised in ~1% of the
212 population), despite being flanked by two *att* sites (Rao et al., 2016). The sequence of the LME-1 *att*
213 site is identical to the *L. pneumophila dif* site, but only encompasses 22-bp of it. Recombination
214 between this 22-bp sequence and the chromosomal *dif* site results in *att*-site duplication, which
215 generates an intact *dif* site upstream and a modified *dif* site downstream of LME-1 that contains 3
216 substitutions (**Fig. 5B**). We next asked whether these modifications to the downstream *dif* site
217 contribute to the stability of the integrated form of LME-1. To address this, we developed an
218 excision assay in which a kanamycin-resistance cassette was used as a proxy for LME-1 by inserting
219 it into the Lp02 Δ*lpg1867*

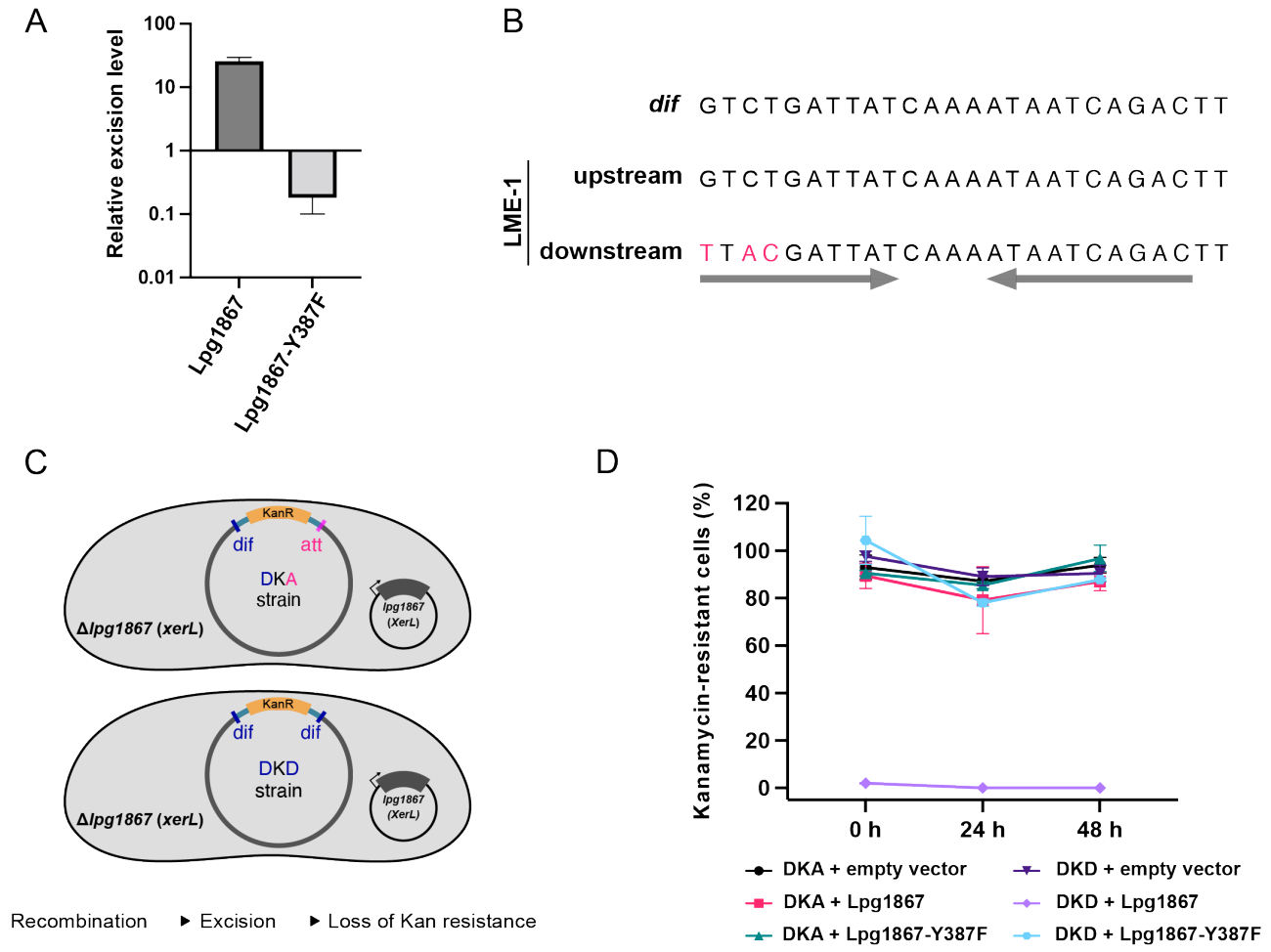

Figure 5 | The sequence of the LME-1 *att* site contributes to its low level of excision, which increases upon Lpg1867 (XerL) overexpression. A) Shown is the effect of overexpression of wildtype Lpg1867 or the catalytic mutant Lpg1867-Y387F on LME-1 excision compared to an empty vector control in *L. pneumophila* strain Murcia-4983. The change in LME-1 excision was determined using an established qPCR-based assay. **B)** Comparison of the wildtype *dif* site in strain Murcia-4983 and the sequences flanking LME-1 resulting from *att* site duplication upon integration into the chromosome. The upstream copy of the *dif* site remains intact, but the downstream copy has three nucleotide differences (pink letters). These differences are within the inverted repeat regions of the *dif* site (denoted by the grey arrows), which presumably contain binding sites for Lpg1867 (XerL). **C)** Schematic representation of the intramolecular recombination assay used to assess the effect of flanking sequencing on LME-1 excision. Wildtype and mutant Lpg1867 expression plasmids were transformed into two strains made in an Δ*lpg1867* background: a *dif*-KanR-*att* (DKA) strain in which the KanR gene is flanked by the sites typically flanking LME-1, and a *dif*-KanR-*dif* (DKD) strain in which the same reporter is flanked by two wildtype *dif* sites. Recombination between the two sites leads to excision of the KanR reporter, which is quantified by plating on selective and nonselective media. **D)** The percent of cells with kanamycin resistance prior to induction of Lpg1867 (wildtype or mutant) and after 24 and 48 hours are plotted. A loss in kanamycin resistance corresponds to recombination between the two sites flanking the KanR reporter. The only strain with significant loss of kanamycin resistance was the DKD strain with wildtype Lpg1867 overexpressed, in which only ~2% of cells maintained the reporter even prior to induction (likely due to leaky expression of Lpg1867 from the plasmid).

220 strain at the *dif* site (**Fig. 5C**). We made two strains: a *dif*-KanR-*att* (DKA) strain in which the KanR
221 gene is flanked by the sites typically flanking LME-1, and a *dif*-KanR-*dif* (DKD) strain in which the
222 same reporter is flanked by two wildtype *dif* sites. We then overexpressed wildtype or mutant
223 Lpg1867 in both of these strains. To quantify excision of the reporter, we determined the proportion
224 of kanamycin-resistant cells in the population prior to induction of expression and at 24-h and 48-h
225 post induction by colony counting on selective and nonselective plates. We found that the LME-1-
226 like reporter in the DKA strain was remarkably stable, even when wildtype Lpg1867 was
227 overexpressed (**Fig. 5D**). In contrast, kanamycin resistance was lost in the vast majority (98%) of
228 cells in the DKD strain containing the wildtype Lpg1867 expression plasmid, even prior to induction
229 (likely due to leaky expression), and no kanamycin-resistant cells remained after 24 h. However, no
230 excision was detected in the DKD strain containing the catalytic mutant Lpg1867 expression
231 plasmid (**Fig. 5D**). The stability of the reporter in the DKA strain suggests that the short 22-bp *att*
232 site of LME-1 likely contributes to the stability of its integrated form by preventing it from being
233 flanked by two intact *dif* sites.
234

235 **DISCUSSION**

236 The discovery of the *L. pneumophila* CDR system has solved two mysteries of the
237 pathogen's biology: the function of the conserved DNA sequence that is hijacked by LME-1, and
238 how *Legionella* species are able to resolve chromosome dimers despite having no homologs to
239 known *dif* sites and Xer recombinases. Similarly, no *dif*/Xer components have been identified in
240 members of the other *Legionellales* family, *Coxiellaceae* (Carnoy & Roten, 2009), which includes
241 the human pathogen *Coxiella burnetii*. A priority going forward will be to characterize the CDR
242 pathway(s) in *Coxiellaceae* using *L. pneumophila* as a genetically tractable surrogate.

243 The *Legionella dif*/Xer system is distinct in several ways from those characterized in other
244 species. The *dif* site arms are a 10-bp inverted repeat with no interruptions, whereas other *dif* sites
245 show only partial dyad symmetry between the two arms, even for single-recombinase systems.
246 Additionally, *dif* and *xerL* are separated by >400 kb in the *L. pneumophila* genome, whereas in the
247 other bacterial single-recombinase systems (*i.e. dif*SL/XerS of *Streptococci* and *Lactococci* and
248 *difH*/XerH of *Campylobacter* and *Helicobacter*), the *dif* site is always near the *xer* gene, indicating
249 they may have been acquired as a single module (Carnoy & Roten, 2009; Castillo et al., 2017; Le
250 Bourgeois et al., 2007; Leroux et al., 2013).
251 With no apparent *dif* or Xer homologs in *Legionella*, the CDR system was instead unearthed
252 through our investigation of LME-1 and its attachment site. In turn, the discovery of the *Legionella*
253 *dif* site and XerL has allowed us to explore new LME-1 biology. We found that the 22-bp LME-1 *att*
254 site is sufficient for integration of circular DNA at the *L. pneumophila dif* site, and that
255 overexpression of XerL boosts LME-1 excision 25-fold. These findings are consistent with LME-1
256 belonging to the IMEX class of integrative mobile elements, which exploit the host CDR machinery
257 for integration and in some cases excision (Das et al., 2013; Midonet & Barre, 2014). The
258 mechanistic details of LME-1 integration and excision, and how they relate to the strategies of other
259 IMEXs, are interesting topics of future study. One intriguing aspect of LME-1 is the stability of its
260 integrated form. Our reporter excision assay showed that the modified *dif* site and wildtype *dif* site
261 that flank the integrated LME-1 do not recombine with each other, or at least recombine at a very
262 low level that is not detectable in our assay. Another stably integrated IMEX, the gonococcal
263 genomic island (GGI) of *Neisseria gonorrheae*, generates a similarly modified *dif* site (dif_{GGI}) at one
264 end of its integrated form, while the wildtype *dif* (dif_{Ng}) remains intact at the other (Fournes et al.,
265 2016). The *Neisseria* CDR system uses XerC and XerD homologs, and recombination takes place

266 when the FtsK DNA translocase pauses at the *dif*/Xer complex and activates XerD. Interestingly,
267 FtsK does not stop at the dif_{GGI}-XerC/D complex, but rather translocates through it, which likely
268 leads to disassembly of the complex and precludes recombination between the dif_{NG} *and* dif_{GGI}
269 (Fournes et al., 2016). It is possible that this same FtsK-dependent process contributes to the stability
270 of the integrated form of LME-1, although we have yet to determine whether XerL requires FtsK for
271 activation. Addressing both of these questions is a priority for our future investigation of the *L.*
272 *pneumophila* CDR system and its associated IMEX, LME-1.

273 The importance of resolving chromosome dimers for the maintenance of genomic stability
274 means that the *dif* site and Xer recombinases are highly conserved (Carnoy & Roten, 2009; Kono et
275 al., 2011), making them an attractive target for integration by IMEXs. The diversity of IMEX
276 elements suggests that *dif*/Xer is a pathway that has been hijacked independently across a broad
277 range of bacteria (Das et al., 2013; Midonet & Barre, 2014), even in a system as distinct as the one in
278 *Legionella.* The discovery of the *Legionella dif*/Xer pathway and its associated IMEX, which had
279 been missed in homology-based searches due to divergence from known CDR components, warrants
280 a closer look at other bacteria in which no *dif*/Xer system has been identified to date.

281

282 **MATERIALS AND METHODS**

283 **Bacterial strains and plasmids**

284 The *L. pneumophila* Lp02 strain was used as the background for all *L. pneumophila* strains
285 generated in this study. The *L. pneumophila* Murcia-4983 strain, which harbors LME-1, is an
286 environmental isolate collected during the 2001 outbreak in Murcia, Spain (García-Fulgueiras et al.,
287 2003). All *L. pneumophila* strains were grown at 37°C in N-(2-acetamido)-2-aminoethanesulfonic

288 acid (ACES) buffered yeast extract supplemented with 100 ug/mL thymidine (AYET) and on
289 charcoal AYET (CYET) agar plates.

290 Deletion strains were made using a scar-free suicide-cassette method described recently
291 (Bailo et al., 2019) with some minor modifications. Briefly, linear DNA containing a mazF-KanR
292 cassette flanked by ~1.5-kb homology arms was introduced into the parental strain via natural
293 transformation. Cells in which the gene of interest had been replaced with the mazF-KanR cassette
294 via homologous recombination were selected by plating on media containing kanamycin. As mazF
295 gene expression is under an IPTG-inducible promoter, colonies can be screened on kanamycin- and
296 IPTG-containing plates to identify cells that are IPTG-sensitive and kanamycin-resistant. In a second
297 natural transformation, linear DNA containing only the homology arms (resulting in gene deletion)
298 was introduced, and cells in which the cassette was excised were selected on plates containing IPTG.
299 Colonies were then screened to identify those that were IPTG-resistant and kanamycin-sensitive, and
300 the deletion was verified by PCR screening and Sanger sequencing.

301 The reporter strains used for the intramolecular recombination (reporter excision) assays
302 were generated by introducing linear DNA containing the *dif*-KanR-*dif* or *dif*-KanR-*att* cassette
303 (flanked by ~1.5 kb homology arms around the chromosomal *dif* site) into the Lp02 Δ*lpg1867* strain.
304 Strains containing the cassette were selected on plates containing kanamycin, and the correct
305 integration of the cassettes was verified by Sanger sequencing.

306 The pJB4648-based plasmids used for the intermolecular recombination assays were
307 constructed by cloning the 22-bp *att* site sequence, a control 22-bp sequence, or 2200 bp of
308 intergenic Lp02 sequence into pJB4648 digested with XhoI and ApaI. The gentamicin-resistant
309 plasmid pJB1806-GmR was generated by first amplifying the gentamicin resistance gene and
310 promoter from pJB4648 and cloning it in place of the chloramphenicol resistance gene in plasmid
311 pJB1806. Protein expression plasmids used for the intermolecular recombination and colony size
312 assays were made by cloning the *lpg1867* gene (wildtype or modified to encode the Y387F

313 mutation) into the multiple cloning site of pNT562 (Nishida et al., 2017). The tet-on-pJB1806-GmR-
314 based expression plasmids used for the reporter excision assays were generated by replacing the
315 *lacIq* gene and tac promoter in pJB1806-GmR with the *tetR* gene and tetracycline-responsive
316 promoter from pLJR965 (Rock et al., 2017) and then cloning in the wildtype or mutant Lpg1867
317 ORF immediately after the promoter, as described by Rock and colleagues (Rock et al., 2017).
318

319 **GC-skew analysis**

320 The cumulative GC-skew maximum value for each *Legionella* genome (shown in Table S1)
321 was determined using the GenSkew java app (https://genskew.csb.univie.ac.at) with default settings.
322 The whole-genome GC-skew profiles and *att* site locations for seven *L. pneumophila* isolates and
323 seven *Legionella* species, selected to show a range of cGC-skew maxima locations relative to the
324 origin, were plotted using Circos (Krzywinski et al., 2009). The GC-skew profiles of these genomes
325 were normalized for genome length. The selected *L. pneumophila* isolates and *Legionella* species
326 are: *L. pneumophila*: Philadelphia_2 (GenBank accession number CP015929.1), Philadelphia_1
327 (AE017354.1), E7_O (CP015954.1), Paris (CR628336.1), NY23 D-7705 (CP021261.1),
328 NCTC11985 (LT906452.1), and subsp. fraseri strain D-4058 (CP021277); *Legionella* species: *L.*
329 *israelensis* L18-01051 (CP041668.1), *L. micdadei* (LN614830.1), *L. spiritensis* NCTC11990
330 (LT906457.1), *L. sainthelensi* NCTC12450 (LR134178.1), *L. longbeachae* NSW150 (FN650140.1),
331 *L. oakridgensis* NCTC11531 (LR134286.1), and *L. fallonii* LLAP-10 (LN614827.1).
332

333 **Recombination assays**

334 For the intermolecular recombination (plasmid integration) assays, each strain was
335 transformed with a pJB4648-based plasmid containing the 22-bp *att* site sequence, a control 22-bp
336 sequence, or 2200 bp sequence as indicated. The strains were also transformed with the replicative
337 plasmid pJB1806-GmR to control for strain-to-strain differences in general transformation

338 efficiency. Plasmid concentrations were determined using a Quant-iT PicoGreen dsDNA kit
339 (Invitrogen), and 200 ng of each plasmid was electroporated into 2 ODU of *L. pneumophila* Lp02
340 cells as described previously (Rao et al., 2013). After an 8-h recovery in liquid AYET media shaking
341 at 37°C, dilutions of each sample were plated onto CYET plates supplemented with 15 µg/mL
342 gentamicin and incubated at 37°C for 4 days. Colonies were counted using GeneTools analysis
343 software (Syngene), and the results were plotted using GraphPad Prism version 9.2.0.
344 For the intramolecular recombination assay, the DKA and DKD strains containing the
345 kanamycin-resistance cassette were transformed with tet-on-pJB1806-GmR containing wildtype
346 Lpg1867, Lpg1867-Y387F, or empty vector by electroporation as described above. Transformants
347 were maintained on CYET plates containing both gentamicin and kanamycin until induction of
348 protein overexpression. Two-day old patches were resuspended in AYET supplemented with
349 gentamicin only, and an aliquot was taken for 0-h timepoint (no induction) CFU counting on
350 selective (CYET+kan) and nonselective (CYET) plates. Liquid cultures were made from the
351 resuspended patches in 2 mL of AYET supplemented with gentamicin and anhydrotetracycline (100
352 ng/mL) at a starting OD_{600} of 0.2, and incubated with shaking at 37°C. After 24 h, each sample was
353 plated for CFU counting and also back-diluted to OD 0.2 for further incubation. At the 48-h
354 timepoint, a final CFU plating was performed. The number of colonies that grew on CYET+kan
355 were compared to the number that grew on CYET to determine the proportion of cells that had lost
356 kanamycin resistance. The results were plotted using GraphPad Prism version 9.2.0.
357
358 **Fluorescent microscopy**
359 Overnight cultures of Lp02, Lp02*Δdif*, Lp02*Δlpg1867*, and Lp02*Δlpg1867ΔrecA* were grown
360 from a 2-day old patch in AYET medium. Bacteria were collected at post-exponential phase (OD_{600}
361 4.0 to 4.5). Approximately ~$1x10^6$ cells (1 ODU) from each strain were washed once with 1 mL of
362 1X PBS before a final resuspension in 500 uL of 1X PBS. The bacteria were stained with 15 µg/mL

363 of DAPI (Roche) for 30 minutes at room temperature and imaged using a 63x oil immersion lens on
364 a Zeiss Axio Imager.M2 microscope.
365
366 **Colony size assay**
367 The distribution of colony size was determined by resuspending 2-day-old patches of the
368 various strains in AYET. The OD_{600} of each cell suspension was determined, and the appropriate
369 dilutions made so that ~200-300 cells were added to each plate. Spread plates were incubated at 37°C
370 for 4 days before imaging using a SynGene system with GeneSnap software (Syngene). Colony
371 diameter was determined using ColTapp automated image analysis software (Bär et al., 2020), and
372 plotted using GraphPad Prism version 9.2.0.
373
374 **Quantitative PCR analysis of LME-1 excision**
375 The quantitative PCR (qPCR) analysis of LME-1 excision was performed as described by
376 Rao and colleagues with some slight modifications (Rao et al., 2016). Briefly, overnight cultures of
377 *L. pneumophila* str. Murcia-4983 carrying either a pNT562 plasmid, a pNT562 plasmid expressing
378 Lpg1867 or a pNT562 plasmid expressing Lpg1867-Y387F were grown from a 2-day-old patch in
379 AYE medium supplemented with 20 µg/mL of kanamycin and 500 µM of IPTG. Bacteria were
380 collected at post-exponential phase (OD_{600} 4.0 to 4.5) and genomic DNA was extracted using a
381 NucleoSpin Tissue Kit (Machery-Nagel) and quantified using a Quant-iT PicoGreen dsDNA kit
382 (Invitrogen). LME-1 excision was quantified by qPCR using SsoAdvanced Universal SYBR Green
383 Supermix (BioRad) and a CFX96 Real-Time System (BioRad). Plasmids containing the
384 amplification products were used as standards for the standard curve. All excision quantifications
385 were done for three biological replicates of each isolate. The excision frequency for each isolate was
386 calculated as described by Rao and colleagues using the following formula (Rao et al., 2016):

387 Excision Frequency = $\frac{Amplicon\ (chrF\&chrR)}{Amplicon\ (chrF\&chrR) + [Amplicon\ (chrF\&lmeR) + Amplicon(lmeF\&chrR)]\ /\ 2}$

388

389 **ACKNOWLEDGEMENTS**

390 We thank members of the Ensminger laboratory for their suggestions and careful reading of the
391 manuscript, and Jordan Lin and John MacPherson for their technical help with the recombination
392 assays. SRD is supported by a fellowship from the Department of Biochemistry, University of
393 Toronto and an Ontario Graduate Scholarship. This work was supported by a Project Grant from the
394 Canadian Institutes of Health Research (PHT-148819).

395

396 **REFERENCES**

397 Austin, S., Ziese, M., & Sternberg, N. (1981). A novel role for site-specific recombination in
398 maintenance of bacterial replicons. *Cell*, *25*(3), 729–736. https://doi.org/10.1016/0092-
399 8674(81)90180-x

400 Bailo, N., Kanaan, H., Kay, E., Charpentier, X., Doublet, P., & Gilbert, C. (2019). Scar-Free
401 Genome Editing in Legionella pneumophila. *Methods in Molecular Biology (Clifton, N.J.)*,
402 *1921*, 93–105. https://doi.org/10.1007/978-1-4939-9048-1_6

403 Bär, J., Boumasmoud, M., Kouyos, R. D., Zinkernagel, A. S., & Vulin, C. (2020). Efficient
404 microbial colony growth dynamics quantification with ColTapp, an automated image
405 analysis application. *Scientific Reports*, *10*(1), 16084. https://doi.org/10.1038/s41598-020-
406 72979-4

407 Barre, F. X., Søballe, B., Michel, B., Aroyo, M., Robertson, M., & Sherratt, D. (2001). Circles: The
408 replication-recombination-chromosome segregation connection. *Proceedings of the National*
409 *Academy of Sciences of the United States of America*, *98*(15), 8189–8195.
410 https://doi.org/10.1073/pnas.111008998

411 Blakely, G., Colloms, S., May, G., Burke, M., & Sherratt, D. (1991). Escherichia coli XerC
412 recombinase is required for chromosomal segregation at cell division. *The New Biologist*,
413 *3*(8), 789–798.
414 Blakely, G., May, G., McCulloch, R., Arciszewska, L. K., Burke, M., Lovett, S. T., & Sherratt, D. J.
415 (1993). Two related recombinases are required for site-specific recombination at dif and cer
416 in E. coli K12. *Cell*, *75*(2), 351–361. https://doi.org/10.1016/0092-8674(93)80076-q
417 Carnoy, C., & Roten, C.-A. (2009). The dif/Xer Recombination Systems in Proteobacteria. *PLoS*
418 *ONE*, *4*(9), e6531. https://doi.org/10.1371/journal.pone.0006531
419 Castillo, F., Benmohamed, A., & Szatmari, G. (2017). Xer Site Specific Recombination: Double and
420 Single Recombinase Systems. *Frontiers in Microbiology*, *8*.
421 https://doi.org/10.3389/fmicb.2017.00453
422 Clerget, M. (1991). Site-specific recombination promoted by a short DNA segment of plasmid R1
423 and by a homologous segment in the terminus region of the Escherichia coli chromosome.
424 *The New Biologist*, *3*(8), 780–788.
425 Colloms, S. D., Sykora, P., Szatmari, G., & Sherratt, D. J. (1990). Recombination at ColE1 cer
426 requires the Escherichia coli xerC gene product, a member of the lambda integrase family of
427 site-specific recombinases. *Journal of Bacteriology*, *172*(12), 6973–6980.
428 https://doi.org/10.1128/jb.172.12.6973-6980.1990
429 Cortez, D., Quevillon-Cheruel, S., Gribaldo, S., Desnoues, N., Sezonov, G., Forterre, P., & Serre,
430 M.-C. (2010). Evidence for a Xer/dif System for Chromosome Resolution in Archaea. *PLoS*
431 *Genetics*, *6*(10), e1001166. https://doi.org/10.1371/journal.pgen.1001166
432 Das, B., Bischerour, J., & Barre, F.-X. (2011). VGJphi integration and excision mechanisms
433 contribute to the genetic diversity of Vibrio cholerae epidemic strains. *Proceedings of the*
434 *National Academy of Sciences of the United States of America*, *108*(6), 2516–2521.
435 https://doi.org/10.1073/pnas.1017061108

436 Das, B., Martínez, E., Midonet, C., & Barre, F.-X. (2013). Integrative mobile elements exploiting
437 Xer recombination. *Trends in Microbiology*, *21*(1), 23–30.
438 https://doi.org/10.1016/j.tim.2012.10.003
439 Debowski, A. W., Carnoy, C., Verbrugghe, P., Nilsson, H.-O., Gauntlett, J. C., Fulurija, A.,
440 Camilleri, T., Berg, D. E., Marshall, B. J., & Benghezal, M. (2012). Xer recombinase and
441 genome integrity in Helicobacter pylori, a pathogen without topoisomerase IV. *PloS One*,
442 *7*(4), e33310. https://doi.org/10.1371/journal.pone.0033310
443 Deecker, S. R., Urbanus, M. L., Nicholson, B., & Ensminger, A. W. (2021). Legionella pneumophila
444 CRISPR-Cas Suggests Recurrent Encounters with One or More Phages in the Family
445 Microviridae. *Applied and Environmental Microbiology*, *87*(17), e0046721.
446 https://doi.org/10.1128/AEM.00467-21
447 Domínguez, N. M., Hackett, K. T., & Dillard, J. P. (2011). XerCD-Mediated Site-Specific
448 Recombination Leads to Loss of the 57-Kilobase Gonococcal Genetic Island. *Journal of*
449 *Bacteriology*, *193*(2), 377–388. https://doi.org/10.1128/JB.00948-10
450 Duggin, I. G., Dubarry, N., & Bell, S. D. (2011). Replication termination and chromosome dimer
451 resolution in the archaeon Sulfolobus solfataricus. *The EMBO Journal*, *30*(1), 145–153.
452 https://doi.org/10.1038/emboj.2010.301
453 Farrokhi, A., Liu, H., & Szatmari, G. (2019). Characterization of the Chromosome Dimer Resolution
454 Site in *Caulobacter crescentus*. *Journal of Bacteriology*, *201*(24), e00391-19,
455 /jb/201/24/JB.00391-19.atom. https://doi.org/10.1128/JB.00391-19
456 Fournes, F., Crozat, E., Pages, C., Tardin, C., Salomé, L., Cornet, F., & Rousseau, P. (2016). FtsK
457 translocation permits discrimination between an endogenous and an imported Xer/ *dif*
458 recombination complex. *Proceedings of the National Academy of Sciences*, *113*(28), 7882–
459 7887. https://doi.org/10.1073/pnas.1523178113

460 García-Fulgueiras, A., Navarro, C., Fenoll, D., García, J., González-Diego, P., Jiménez-Buñuales,
461 T., Rodriguez, M., Lopez, R., Pacheco, F., Ruiz, J., Segovia, M., Balandrón, B., & Pelaz, C.
462 (2003). Legionnaires' disease outbreak in Murcia, Spain. *Emerging Infectious Diseases*, *9*(8),
463 915–921. https://doi.org/10.3201/eid0908.030337
464 Gibb, B., Gupta, K., Ghosh, K., Sharp, R., Chen, J., & Van Duyne, G. D. (2010). Requirements for
465 catalysis in the Cre recombinase active site. *Nucleic Acids Research*, *38*(17), 5817–5832.
466 https://doi.org/10.1093/nar/gkq384
467 Grigoriev, A. (1998). Analyzing genomes with cumulative skew diagrams. *Nucleic Acids Research*,
468 *26*(10), 2286–2290. https://doi.org/10.1093/nar/26.10.2286
469 Hassan, F., Kamruzzaman, M., Mekalanos, J. J., & Faruque, S. M. (2010). Satellite phage TLCφ
470 enables toxigenic conversion by CTX phage through dif site alteration. *Nature*, *467*(7318),
471 982–985. https://doi.org/10.1038/nature09469
472 Hendricks, E. C., Szerlong, H., Hill, T., & Kuempel, P. (2000). Cell division, guillotining of dimer
473 chromosomes and SOS induction in resolution mutants (dif, xerC and xerD) of Escherichia
474 coli. *Molecular Microbiology*, 9.
475 Huber, K. E., & Waldor, M. K. (2002). Filamentous phage integration requires the host
476 recombinases XerC and XerD. *Nature*, *417*(6889), 656–659.
477 https://doi.org/10.1038/nature00782
478 Jensen, R. B. (2006). Analysis of the terminus region of the Caulobacter crescentus chromosome and
479 identification of the dif site. *Journal of Bacteriology*, *188*(16), 6016–6019.
480 https://doi.org/10.1128/JB.00330-06
481 Kono, N., Arakawa, K., & Tomita, M. (2011). Comprehensive prediction of chromosome dimer
482 resolution sites in bacterial genomes. *BMC Genomics*, *12*(1), 19.
483 https://doi.org/10.1186/1471-2164-12-19

484 Krzywinski, M., Schein, J., Birol, I., Connors, J., Gascoyne, R., Horsman, D., Jones, S. J., & Marra,
485 M. A. (2009). Circos: An information aesthetic for comparative genomics. *Genome*
486 *Research*, *19*(9), 1639–1645. https://doi.org/10.1101/gr.092759.109
487 Kuempel, P. L., Henson, J. M., Dircks, L., Tecklenburg, M., & Lim, D. F. (1991). Dif, a recA-
488 independent recombination site in the terminus region of the chromosome of Escherichia
489 coli. *The New Biologist*, *3*(8), 799–811.
490 Le Bourgeois, P., Bugarel, M., Campo, N., Daveran-Mingot, M.-L., Labonté, J., Lanfranchi, D.,
491 Lautier, T., Pagès, C., & Ritzenthaler, P. (2007). The Unconventional Xer Recombination
492 Machinery of Streptococci/Lactococci. *PLoS Genetics*, *3*(7), e117.
493 https://doi.org/10.1371/journal.pgen.0030117
494 Leroux, M., Rezoug, Z., & Szatmari, G. (2013). The Xer/dif site-specific recombination system of
495 Campylobacter jejuni. *Molecular Genetics and Genomics*, *288*(10), 495–502.
496 https://doi.org/10.1007/s00438-013-0765-5
497 Lüneberg, E., Mayer, B., Daryab, N., Kooistra, O., Zähringer, U., Rohde, M., Swanson, J., & Frosch,
498 M. (2001). Chromosomal insertion and excision of a 30 kb unstable genetic element is
499 responsible for phase variation of lipopolysaccharide and other virulence determinants in
500 Legionella pneumophila. *Molecular Microbiology*, *39*(5), 1259–1271.
501 https://doi.org/10.1111/j.1365-2958.2001.02314.x
502 Midonet, C., & Barre, F.-X. (2014). Xer Site-Specific Recombination: Promoting Vertical and
503 Horizontal Transmission of Genetic Information. *Microbiology Spectrum*, *2*(6).
504 https://doi.org/10.1128/microbiolspec.MDNA3-0056-2014
505 Midonet, C., Das, B., Paly, E., & Barre, F.-X. (2014). XerD-mediated FtsK-independent integration
506 of TLCϕ into the Vibrio cholerae genome. *Proceedings of the National Academy of Sciences*
507 *of the United States of America*, *111*(47), 16848–16853.
508 https://doi.org/10.1073/pnas.1404047111

509 Nishida, T., Watanabe, K., Tachibana, M., Shimizu, T., & Watarai, M. (2017). Characterization of
510 the cryptic plasmid pOfk55 from Legionella pneumophila and construction of a pOfk55-
511 derived shuttle vector. *Plasmid*, *90*, 30–37. https://doi.org/10.1016/j.plasmid.2017.02.004
512 Pan, G., Luetke, K., & Sadowski, P. D. (1993). Mechanism of cleavage and ligation by FLP
513 recombinase: Classification of mutations in FLP protein by in vitro complementation
514 analysis. *Molecular and Cellular Biology*, *13*(6), 3167–3175.
515 Pérals, K., Cornet, F., Merlet, Y., Delon, I., & Louarn, J. M. (2000). Functional polarization of the
516 Escherichia coli chromosome terminus: The dif site acts in chromosome dimer resolution
517 only when located between long stretches of opposite polarity. *Molecular Microbiology*,
518 *36*(1), 33–43. https://doi.org/10.1046/j.1365-2958.2000.01847.x
519 Rao, C., Benhabib, H., & Ensminger, A. W. (2013). Phylogenetic reconstruction of the Legionella
520 pneumophila Philadelphia-1 laboratory strains through comparative genomics. *PloS One*,
521 *8*(5), e64129. https://doi.org/10.1371/journal.pone.0064129
522 Rao, C., Guyard, C., Pelaz, C., Wasserscheid, J., Bondy-Denomy, J., Dewar, K., & Ensminger, A.
523 W. (2016). Active and adaptive *Legionella* CRISPR-Cas reveals a recurrent challenge to the
524 pathogen. *Cellular Microbiology*, *18*(10), 1319–1338. https://doi.org/10.1111/cmi.12586
525 Rock, J. M., Hopkins, F. F., Chavez, A., Diallo, M., Chase, M. R., Gerrick, E. R., Pritchard, J. R.,
526 Church, G. M., Rubin, E. J., Sassetti, C. M., Schnappinger, D., & Fortune, S. M. (2017).
527 Programmable transcriptional repression in mycobacteria using an orthogonal CRISPR
528 interference platform. *Nature Microbiology*, *2*, 16274.
529 https://doi.org/10.1038/nmicrobiol.2016.274
530 Sciochetti, S. A., Piggot, P. J., & Blakely, G. W. (2001). Identification and characterization of the dif
531 Site from Bacillus subtilis. *Journal of Bacteriology*, *183*(3), 1058–1068.
532 https://doi.org/10.1128/JB.183.3.1058-1068.2001

533 Steiner, W. W., & Kuempel, P. L. (1998). Sister chromatid exchange frequencies in Escherichia coli
534 analyzed by recombination at the dif resolvase site. *Journal of Bacteriology*, *180*(23), 6269–
535 6275. https://doi.org/10.1128/JB.180.23.6269-6275.1998
536 Summers, D. K., & Sherratt, D. J. (1984). Multimerization of high copy number plasmids causes
537 instability: CoIE1 encodes a determinant essential for plasmid monomerization and stability.
538 *Cell*, *36*(4), 1097–1103. https://doi.org/10.1016/0092-8674(84)90060-6
539 Thanbichler, M. (2010). Synchronization of Chromosome Dynamics and Cell Division in Bacteria.
540 *Cold Spring Harbor Perspectives in Biology*, *2*(1), a000331–a000331.
541 https://doi.org/10.1101/cshperspect.a000331
542 Val, M.-E., Bouvier, M., Campos, J., Sherratt, D., Cornet, F., Mazel, D., & Barre, F.-X. (2005). The
543 single-stranded genome of phage CTX is the form used for integration into the genome of
544 Vibrio cholerae. *Molecular Cell*, *19*(4), 559–566.
545 https://doi.org/10.1016/j.molcel.2005.07.002
546 Val, M.-E., Kennedy, S. P., El Karoui, M., Bonné, L., Chevalier, F., & Barre, F.-X. (2008). FtsK-
547 dependent dimer resolution on multiple chromosomes in the pathogen Vibrio cholerae. *PLoS*
548 *Genetics*, *4*(9), e1000201. https://doi.org/10.1371/journal.pgen.1000201
549
550
551 **SUPPLEMENTARY MATERIAL:**
552 **Table S1 | The *att* site is close to the cumulative GC-skew maximum in all sequenced *L.***
553 ***pneumophila* strains and *Legionella* species.** The nucleotide positions of the *att* site and cumulative
554 GC-skew maximum (cGC skew max) are shown for each *L. pneumophila* strain and *Legionella*
555 species with a completed genome sequence available in Genbank. The cGC skew maximum
556 corresponds to the site of replication termination (Grigoriev, 1998). The genes immediately upstream
557 and downstream of each *att* site are also indicated.